


# Robust Anti-Jamming Algorithm Based on Transmit/Receive Time-Sharing Technology

Baiyu Li <sup>1</sup>, Zukun Lu <sup>1,\*</sup> , Jie Song <sup>1,\*</sup>, Wei Xiao <sup>1</sup>, Jia Qiao <sup>1</sup>, Long Huang <sup>1</sup>, Zhibin Xiao <sup>1</sup> and Baojun Lin <sup>2</sup>

<sup>1</sup> College of Electronic Science and Technology, National University of Defense Technology, Changsha 410073, China

<sup>2</sup> Innovation Academy for Microsatellites of Chinese Academy of Sciences, Shanghai 201203, China

\* Correspondence: luzukun@nudt.edu.cn (Z.L.); songjie16@nudt.edu.cn (J.S.);

Tel.: +86-155-7499-3958 (Z.L.); +86-151-1624-8471 (J.S.)

**Abstract:** Transmit/Receive (T/R) time-sharing is a critical technology to ensure accurate space–time reference information of navigation signals, which solves the problem of co-channel interference between receiver and transmitter. The rapid development of the electronic information industry has led to severe frequency band conflicts between different electronic systems. Satellite navigation receivers must take measures to suppress interference to eliminate the effects of narrowband interference, mainly unintentional interference. Time-domain anti-jamming is widely used in navigation receivers for its simple and easy advantages in ensuring the validity and stability of navigation data. However, because the satellite-ground link receivers adopt transmit/receive time-sharing technology to realize the bidirectional measurement and communication function of the link, the stability of the data solution is greatly affected by anti-interference in the time domain. The anti-jamming filter of the traditional navigation receiver usually re-converges from the initial state in each signal-receiving time slot, which leads to the receiver losing high volume data due to repeated convergence. This paper proposes a robust time-domain anti-jamming technology based on transmit/receive time-sharing technology. The continuity and stability of the interference signal are used to obtain the preliminary information of the periodic transceiver. The results show that robust anti-jamming technology based on a T/R time-sharing navigation signal can effectively improve the carrier-to-noise ratio loss and data loss caused by traditional time-domain anti-jamming technology, reduce the convergence time to nanosecond level, and has bright prospects in the future application of other navigation systems.

**Keywords:** BeiDou Navigation Satellite System; transmit/receive time-sharing; time-domain anti-jamming; robust anti-jamming algorithm



**Citation:** Li, B.; Lu, Z.; Song, J.; Xiao, W.; Qiao, J.; Huang, L.; Xiao, Z.; Lin, B. Robust Anti-Jamming Algorithm Based on Transmit/Receive Time-Sharing Technology. *Machines* **2022**, *10*, 952. <https://doi.org/10.3390/machines10100952>

Academic Editor: Giovanni B. Palmerini

Received: 8 September 2022

Accepted: 17 October 2022

Published: 19 October 2022

**Publisher's Note:** MDPI stays neutral with regard to jurisdictional claims in published maps and institutional affiliations.



**Copyright:** © 2022 by the authors. Licensee MDPI, Basel, Switzerland. This article is an open access article distributed under the terms and conditions of the Creative Commons Attribution (CC BY) license (<https://creativecommons.org/licenses/by/4.0/>).

## 1. Introduction

The Global Navigation Satellite System (GNSS) has become a critical infrastructure to promote the development of global economic society, and in modern high-tech warfare [1]. GNSS provides spatiotemporal information, which is widely used in communication, finance, multimedia, and so on [2]. While providing navigation and positioning functions, navigation receivers are highly susceptible to interference [3,4]. The rapid development of various electronic systems has resulted in overlapping in the electromagnetic spectrum [5]. Because of the minimal ground arrival power of the navigation signal and the limited anti-interference margin of navigation receivers, the unintentional interference represented by the electromagnetic signals of other electronic systems significantly impacts the navigation receiver [6,7]. For example, there are conflicts between the Global Positioning System (GPS) utilization of civil aviation airports and drones, which results in many conflict events [8,9]. Anti-jamming technology has become an essential research topic in the field of satellite navigation [10].

Time-domain anti-jamming technology is one of the most effective ways to suppress narrowband interference [11]. It is widely used in tiny navigation receivers such as hand-sets because of its simple and easy implementation [12,13]. The anti-jamming module receives the digital signal through the radio-frequency front-end (RFFE) and transmits the processed data to the receiver back-end, suppressing narrowband interference and ensuring navigation signal availability [14,15]. Compared to the recursive least square (RLS), Levinson–Durbin, and Burg algorithms, the least mean squares (LMS) algorithm has become one of navigation receivers’ most commonly used NBI suppression techniques [16,17].

Transmit/receive (T/R) time-sharing is a critical technology to provide precise space-time reference information for satellite-ground link receivers [18,19]. The receiver alternately sends and receives signals in the T/R time-sharing period and performs bidirectional measurement and communication with the satellite receiver or the ground station [20]. The signal reception interval is usually shorter than the duration of narrowband interference. Therefore, in traditional BeiDou navigation receivers, there are multiple T/R time-sharing periods in the interference duration, and the anti-interference filter re-converges from the initial state whenever the T/R time-sharing cycle restarts.

In the non-convergence stage of the anti-jamming filter, the navigation receiver cannot perform signal calculation, typically because the signal quality cannot reach the acquisition and tracking sensitivity of the receiver, resulting in the loss of information of the navigation signal [21,22]. The classic navigation receiver usually receives a continuous signal directly, and the traditional anti-jamming algorithm is also designed for this kind of scenario. However, due to the emergence of T/R time-sharing technology, the navigation receiver sends and receives signals periodically. The traditional anti-jamming algorithm will have a long non-convergence time each time the signal is received, and a lot of information will be lost in the non-convergence stage [23], which seriously affects the actual performance of the navigation receiver. Therefore, to solve this problem has become an important research topic in the literature on T/R time-sharing receiver technology. However, there is no research on this problem which can be directly applied to the navigation receiver.

Observing the characteristics of the interference signal, the signal is stable compared to navigation signals that change randomly in different periods [24]. Therefore, the idea of this paper is to generate preliminary information according to interference characteristics to solve the problem of data loss caused by filter re-convergence.

This paper presents a robust time-domain anti-jamming algorithm based on T/R time-sharing technology. The prior information is generated using the persistence and stability of interference, which provides the initial data for the anti-jamming filter. Section 2 describes the mathematical model of T/R time-sharing and the time-domain anti-jamming filter. Section 3 analyzes the influence of time-domain anti-interference on T/R time-sharing performance. Section 4 introduces the robust anti-jamming algorithm based on T/R time-sharing technology and analyzes its performance. Section 5 verifies the robust anti-jamming algorithm in different interference and signal scenarios. Finally, the algorithm is summarized.

## 2. Mathematical Model

### 2.1. Transmit/Receive Time-Sharing Model

The satellite-ground link receiver of the BeiDou Navigation Satellite System (BDS) realizes bidirectional measurement and communication through T/R time-sharing technology [25,26]. The T/R time-sharing module is illustrated in Figure 1. The time-sharing period of the satellite-ground link is 3 s [27]. Both the signal receiving and transmitting time slots are 1.5 s. When the navigation receiver communicates with the linked satellite, it first receives the downlink signal from the navigation satellite and then transmits new data to the satellite. The signal reception interval of the navigation receiver on the satellite-ground link can be expressed as:

$$T_r = \min|t_{i,j} - t_{j,i}| = 1.5 \text{ s} \quad (1)$$

where,  $t_{i,j}$  is the signal receiving time from transmitter  $i$  to receiver  $j$ .

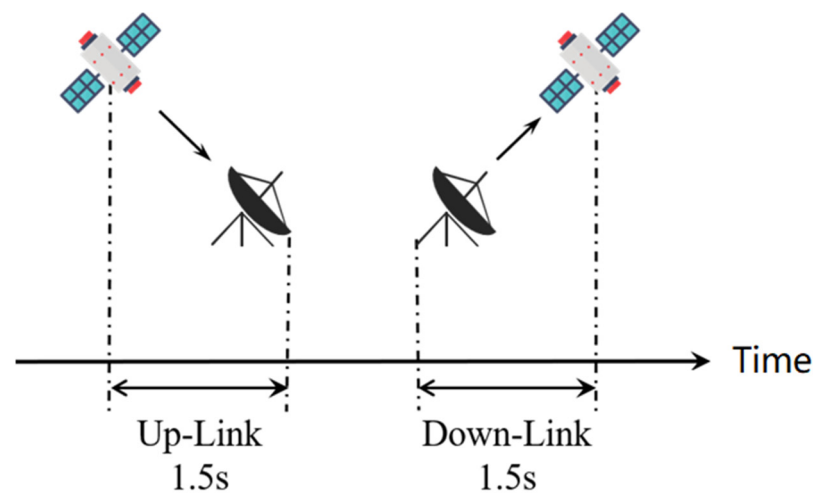


**Figure 1.** Transmit/receive time-sharing model of satellite-ground link.

In the non-receiving interval, the navigation receiver stops performing the signal reception function, but the interference environment still exists [28]. Figure 2 illustrates the time-domain diagram of the received signal in the anti-jamming module. As shown in the figure, the navigation signals in different time-sharing periods are different satellite downlink signals, but the interference environment remains the same, showing the same characteristics.

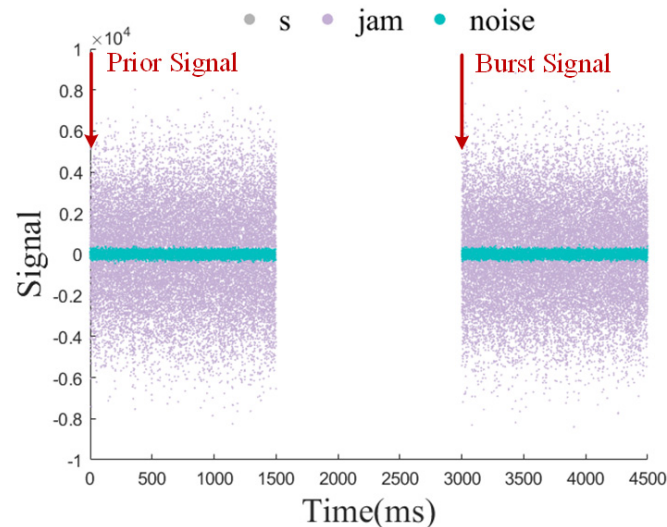


**Figure 2.** Time-domain diagram of the received signal.

## 2.2. Time-Domain Anti-Jamming Model

Time-domain anti-jamming is a necessary baseband digital signal processing (DSP) module of the navigation receiver, as shown in Figure 3 [29,30]. Among them, the LMS adaptive filter is an important anti-jamming method in the time domain, which can be independently embedded in the receiver with a small size, and its suppression effect on narrowband interference is usually greater than 30 dB [31]. The LMS algorithm uses the steepest gradient descent to minimize the error signal's mean square value, which has the characteristics of small calculation and simple implementation [32].

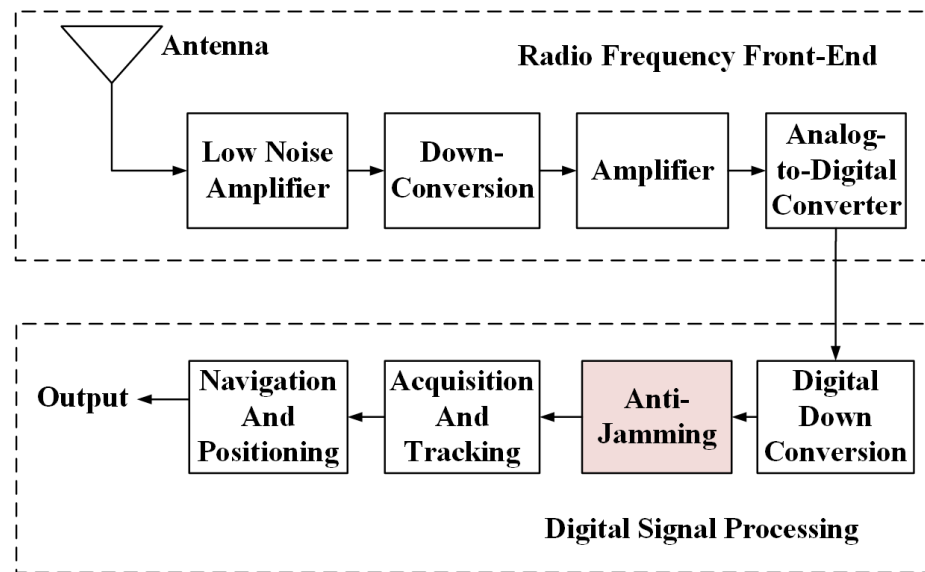


Figure 3. Navigation receiver structure.

Suppose that the intermediate frequency (IF) signal, noise, and interference received from an antenna and processed after DDC are  $s[n]$ ,  $n[n]$  and  $j[n]$ , respectively, and they are all complex signals [33]. Then, the signal before anti-jamming can be expressed as:

$$x[n] = s[n] + j[n] + n[n] \tag{2}$$

The  $M$ -th time-domain filter has  $M + 1$  taps, and the filter weight vector is supposed to be [24]:

$$\mathbf{W}_M = [w_0, w_1, \dots, w_M] \tag{3}$$

The output signal after the anti-jamming filter can be expressed in the time domain as [34]:

$$y[n] = x[n] * \mathbf{W}_M = \sum_{k=0}^M x[n - k] \mathbf{W}_M[k] \tag{4}$$

The frequency response of the anti-jamming filter can be written as [35]:

$$H(f) = \text{DTFT}[\mathbf{W}_M] \tag{5}$$

The error signal between the filter output signal and the input signal is defined as  $e(n)$ , which can be expressed as [36]:

$$e[n] = x[n] - y[n] \tag{6}$$

The adaptive algorithm adjusts the filter tap coefficients according to the error signal and makes the filter weight vector change along the negative gradient direction by iteration [37]:

$$\mathbf{W}_M^{l+1} = \mathbf{W}_M^l - \mu \nabla_{\mathbf{w}_M} E \{ |e[n]|^2 \} \tag{7}$$

where  $l$  is the number of adaptive iterations, and the maximum number of iterations is  $L$ ,  $\mu$  represents the rate at which the gradient is falling.

In practical applications, the instantaneous mean square error is usually used instead of the mean square error, and the recursive formula of the LMS algorithm is finally obtained by substituting the formula [30]:

$$\mathbf{W}_M^{l+1} = \mathbf{W}_M^l + 2\mu e^*[n]x[n] \tag{8}$$

### 3. Influence Analysis of Time-Domain Anti-Jamming on Burst Signal

Convergence time and data loss are essential parameters for evaluating the influence of time-domain anti-jamming on burst signals in the satellite-ground link [20]. In the non-convergence interval, the carrier-to-noise ratio (CNR) cannot satisfy the receiver acquisition sensitivity, resulting in unavailable navigation data. Receiver convergence time and data loss depend on receiver sensitivity [38].

In traditional BeiDou navigation receivers, the time-domain anti-jamming filter presents the characteristics of repeated convergence. The navigation receiver stops working in the non-receiving time slot, and the anti-jamming filter stops iterating and transfers to the initial state. When the receiver enters the following T/R time-sharing period, the filter converges again from the initial weight vector. Figure 4 shows that the convergence time required for the filter weight vector to stabilize is about 5 ms. The time-domain filter order is set to 33, the original CNR is set to 50 dB·Hz, the jamming-to-signal ratio (JSR) is set to 50 dB, and the interference bandwidth is 2 MHz. All subsequent description simulations are completed with the above conditions (Figures 4–6 are based on this).

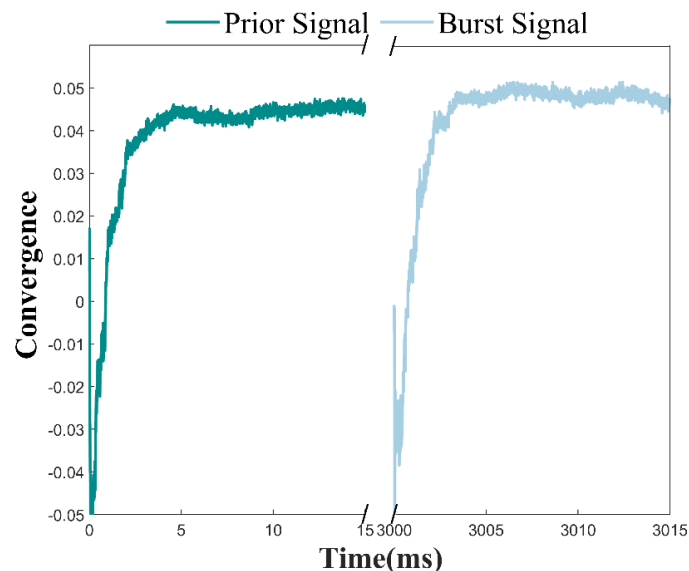


Figure 4. The convergence of the traditional algorithm.

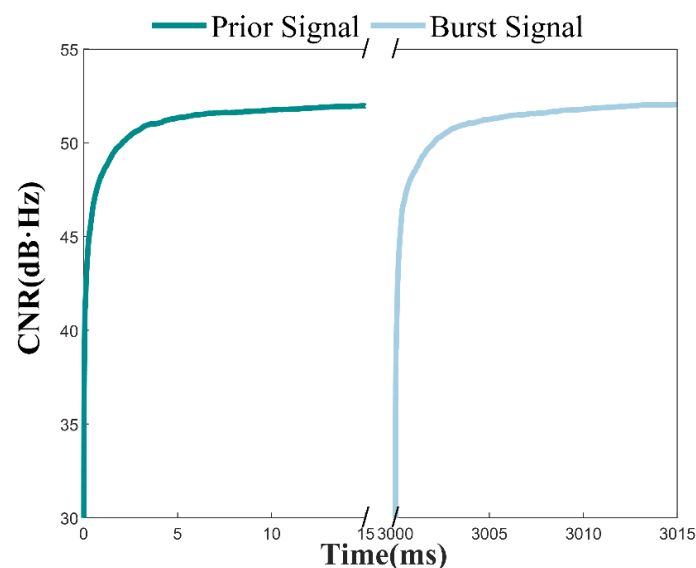


Figure 5. The estimated CNR of the traditional algorithm.

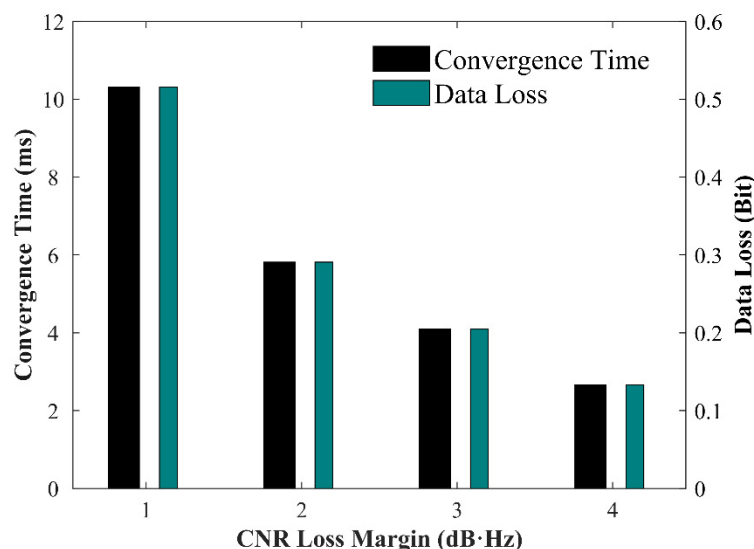


Figure 6. The effect of CNR loss margin on convergence.

The carrier-to-noise ratio is an important parameter to evaluate whether the navigation signal can be calculated. The CNR without interference is the ratio of the average power of the navigation signal to the noise signal [39]:

$$[C/N]_0 = \frac{C}{N} \cdot B_N = \frac{\int_{-\infty}^{\infty} S_s(f)df}{\int_{-\infty}^{\infty} S_n(f)df} \cdot B_n \tag{9}$$

The estimated CNR after anti-jamming is a vital indicator for estimating the interference suppression performance, which can be expressed as:

$$[C/N]_{ajm} = \frac{\int_{-\infty}^{\infty} |H(f)|^2 S_s(f)df}{\int_{-\infty}^{\infty} S_y(f)df - \int_{-\infty}^{\infty} |H(f)|^2 S_s(f)df} \tag{10}$$

where  $S_s(f)$  and  $S_n(f)$  are the power spectral densities of the IF signal and noise, respectively.

When the CNR loss of the output signal is less than the performance requirement, the actual convergence time of the navigation receiver can be calculated:

$$T_{conv} = T \left| [C/N]_0 - [C/N]_{ajm} \right| < \delta \tag{11}$$

where  $\delta$  is the maximum CNR loss satisfying the acquisition sensitivity of the navigation receiver.

Figure 5 illustrates the output CNR variation trend in the interference suppression process. When the CNR loss does not satisfy the receiver sensitivity, no navigation signal can be processed solved in the acquisition and tracking module, and the critical timing and positioning information cannot be calculated. As the filter converges, the data length of the output signal increases, and the estimated CNR gradually approaches the original CNR, unaffected by interference, and tends to be stable.

When the receiver does not converge, the residual interference of the output signal exceeds the anti-interference margin of the receiver, so no data solution is valid in the acquisition and tracking module. Therefore, the repeated convergence of the receiver will cause information loss in each T/R time-sharing period, and the data loss can be expressed as the signal rate within the convergence time [40]:

$$Q_{loss} = T_{conv} R_{code} \tag{12}$$

where,  $R_{code}$  is the code rate, which is 50 bits per second (50 bps).

The actual convergence performance of the anti-jamming filter under different interference suppression margin requirements is shown in Figure 6. When the CNR loss decreases to less than 1 dB·Hz, the filter converges after approximately 10.31 ms. When the CNR loss margin is 4 dB·Hz, only 2.66 ms is required. The diagram shows that the smaller the CNR loss margin of the receiver, the longer convergence time and more significant data loss are caused.

The BDS is still in the demonstration and development stage. For example, the transmit/receive time-sharing technology in low-orbit constellation communications is still under research. In addition to the satellite-ground link with the T/R time-sharing period of 3 s, other system links are still under construction, which may adopt different periods to achieve T/R time-sharing. When the time requirement is less than the satellite-ground link period, the time-domain anti-interference may impact other link burst signal systems more. Figure 7 shows the proportion of data loss under different receiving time slots and analyzes the influence of signal receiving time slots on the signal quality of the navigation receiver. It can be seen from the figure that as the signal reception interval decreases, the receiving quality of the burst navigation signal becomes more affected by anti-interference. As the CNR loss margin of the receiver decreases, the time-domain anti-interference has more apparent damage to the quality of the navigation signal.

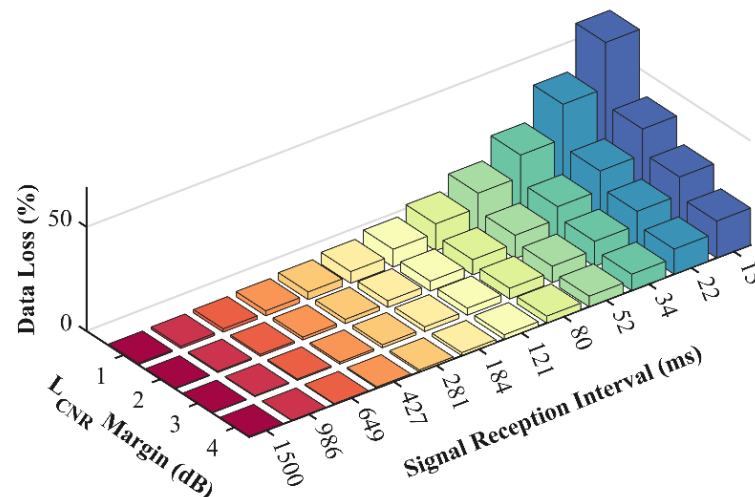


Figure 7. The effect of signal reception interval on data loss.

#### 4. Robust Anti-Jamming Algorithm Based on the Transmit/Receive Time-Sharing

##### 4.1. Robust Anti-Jamming Algorithm

Under long-term continuous interference, there are usually multiple T/R time-sharing periods. Navigation receivers usually receive navigation signals from random satellites in different T/R cycles, but the interference characteristics, such as interference bandwidth, power, and center frequency, are stable. Therefore, the interference characteristics can be used as the preliminary information to provide the initial value for the next re-convergence to ensure that the receiver can quickly converge in the following T/R time-sharing period. The time-domain anti-jamming algorithm of the satellite navigation receiver based on the time-sharing signal system is shown in Figure 8. When the burst signal clock level is 1, the weight memory is enabled and the previous convergence weight is transmitted to the anti-interference module as the initial weight. This is also the innovation of this algorithm.

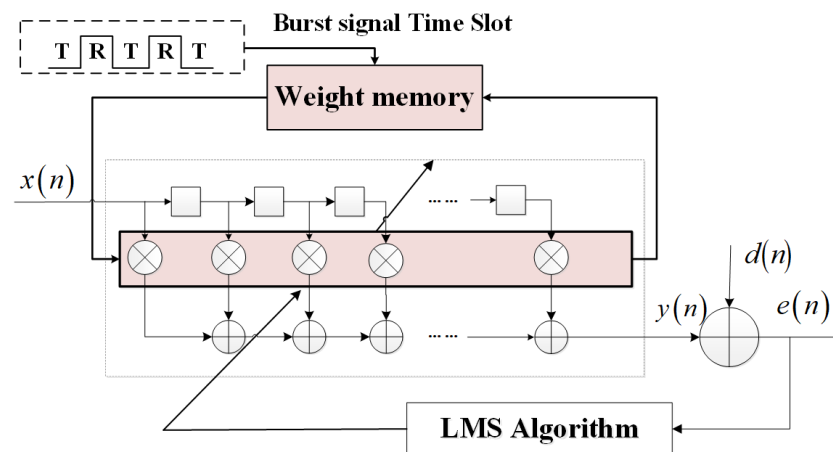


Figure 8. The flow chart of the robust anti-jamming algorithm.

Suppose that the weight vector of the converged anti-jamming filter in the  $i$ -th period is stored and applied to the  $(I + 1)$ -th initial weight vector:

$$W_M^{i+1,1} = W_M^{i,end} \tag{13}$$

The weight convergence of the robust time-domain anti-jamming algorithm is shown in Figure 9. The navigation receiver converges slowly in the preliminary information stage. After entering the next receiving time slot, the filter weight does not increase significantly but achieves rapid convergence and almost no information loss.

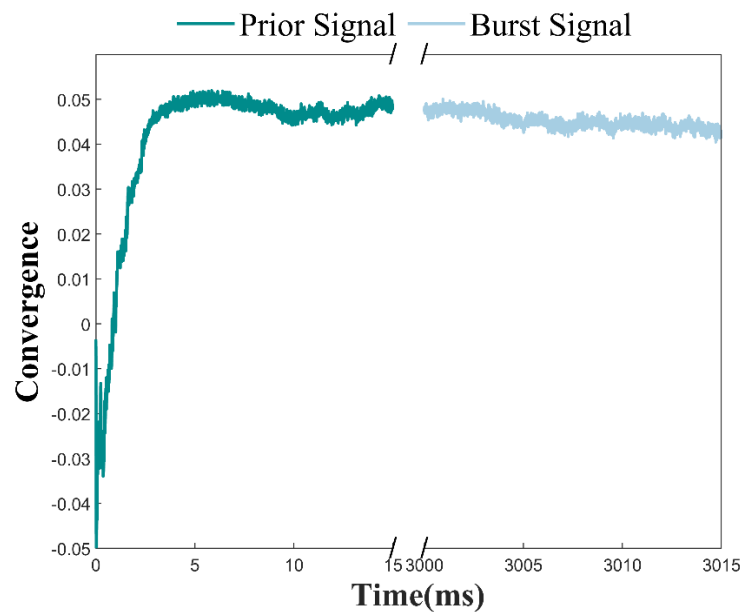
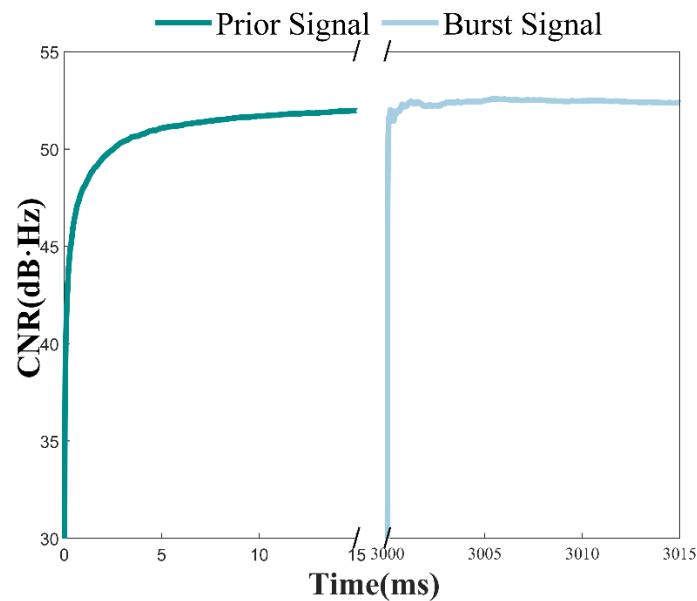


Figure 9. The convergence of the robust anti-jamming algorithm.

The estimated CNR of the prior signal and the burst signal are shown in Figure 10. When the anti-jamming filter converges to stability, the stable value of the filter weight vector can provide a priori information for the burst signal. Therefore, the interference in the subsequent periods can be effectively suppressed once the burst signal is transmitted to the anti-jamming filter. The figure shows that the output estimated CNR increases rapidly, and only 0.0132 ms is required when the CNR loss margin is 1 dB·Hz.





**Figure 10.** The estimated CNR of the robust anti-jamming algorithm.

#### 4.2. Performance Analysis

In order to evaluate the proposed algorithm's performance under different factors, various experiments were carried out for different narrowband interference scenarios. It is assumed that the prior and burst signals are navigation signals from any random B3 satellite, the data length is 15 ms, the sampling rate is 25 MHz, the modulation mode is P code BPSK modulation, and the pseudo-code rate is 10.23 MHz. When analyzing the performance of the anti-jamming receiver, the CNR and convergence time after anti-jamming were considered, and the prospect of the robust anti-jamming algorithm was analyzed for possible application in BDS. Because of the considerable convergence time difference between the robust anti-jamming algorithm and the traditional anti-jamming algorithm, the data is expressed in dB form.

The robust anti-jamming algorithm can improve the problem of increased CNR loss and increased signal loss caused by increased interference intensity. Figure 11 shows the simulation results of robust anti-jamming algorithms under different JSR. The original CNR is set to 55 dB·Hz, and the interference bandwidth is set to 2 MHz. As shown in the figure, the CNR loss in the traditional anti-time-domain interference receiver will gradually increase as the interference power increases. However, the robust anti-jamming filter can use the prior information to converge exceptionally quickly to ensure that the CNR loss is always less than 1 dB·Hz. In addition, the convergence time of the traditional anti-interference algorithm will gradually increase. In contrast, the convergence time of the robust algorithm is around  $-20$  dB less than the traditional one.

The robust anti-jamming algorithm can improve the problem of longer convergence time caused by increased jamming bandwidth. The simulation results of the robust anti-jamming algorithm under different bandwidth interference are shown in Figure 12. The original CNR is set to 55 dB·Hz, and the JSR is set to 45 dB. Results show that the interference bandwidth within the range does not affect the CNR performance between the anti-jamming algorithms, traditional and proposed. However, the information loss shows the advantages of the robust method in the convergence time. The convergence time of the traditional algorithm increases with the increase of interference bandwidth, while the convergence time of the robust anti-jamming algorithm remains at 20 ns.

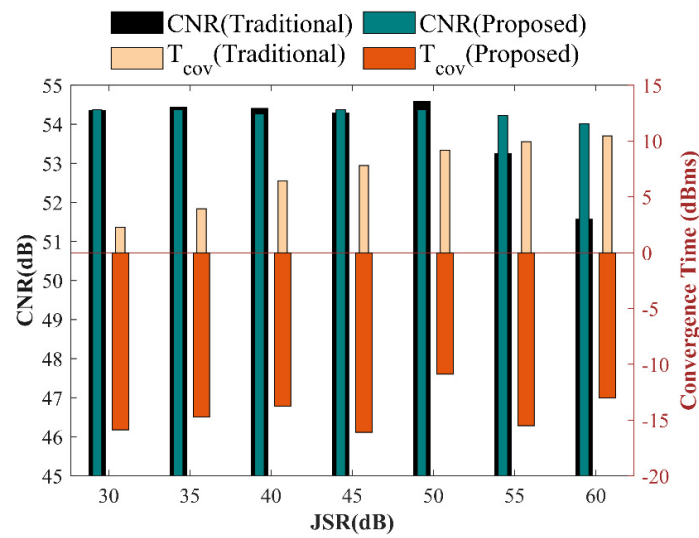


Figure 11. Performance comparison under scenarios with different interference power.

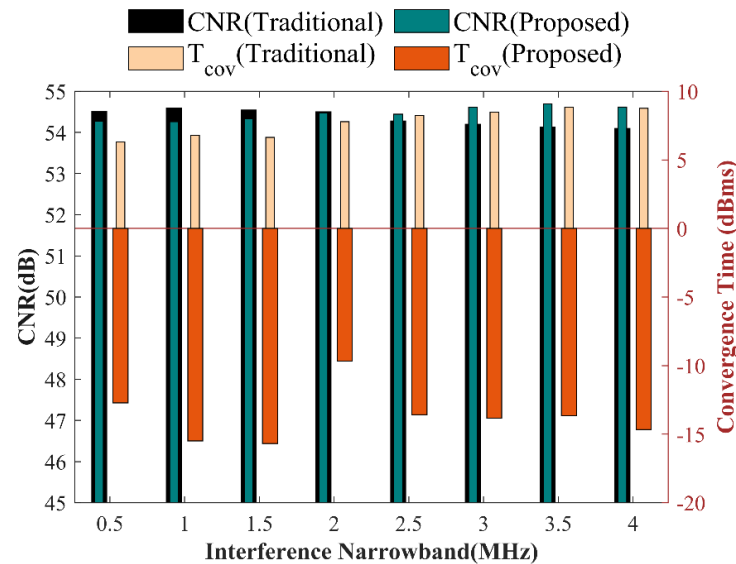


Figure 12. Performance comparison under scenarios with different interference bandwidth.

Under the influence of navigation signal strength, the robust anti-jamming algorithm can improve CNR loss and convergence time increase in strong signal scenarios. Figure 13 shows the simulation results of the robust anti-jamming algorithms under different original CNR scenarios. Assuming that the JSR is 50 dB, and the interference bandwidth is 2 MHz, the anti-interference effect is optimized by adjusting the iteration step. The figure shows that the traditional algorithm in strong signal scenarios will produce a significant CNR loss with a longer convergence time. In contrast, the robust anti-jamming algorithm can achieve a slight CNR loss in a short convergence time. The CNR loss of the proposed algorithm is significantly smaller than the traditional one. Moreover, the advantage of the robust algorithm becomes more evident as the signal power increases.

The application of T/R time-sharing technology in the future BDS has broad prospects. Figure 14 intuitively analyzes the convergence results of the robust anti-jamming algorithm with different signal reception intervals. Considering that 1.5 s navigation data can be sufficiently resolved in navigation receivers, other constellations and link communication may adopt a shorter period to realize the T/R time-sharing technology. Figure 14 analyzes the filter performance when the signal reception intervals are 15 ms and 75 ms, respectively. Figure 14a,c is the interference suppression performance with short reception interval, and

Figure 14b,d is the interference suppression performance with a long reception interval. The convergence performance and CNR in this figure show that T/R time-sharing technology has more obvious advantages for receivers with short reception intervals, which can obtain good performance in dealing with highly dynamic interference [41].

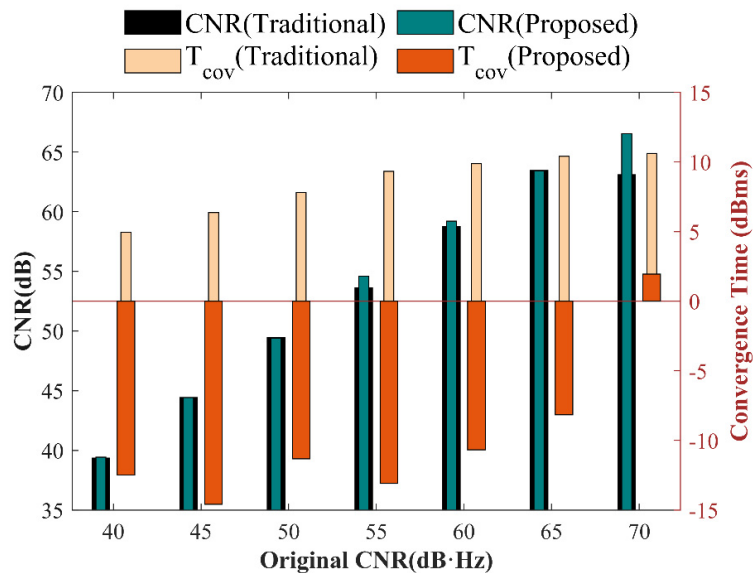


Figure 13. Performance comparison under scenarios with different original CNR.

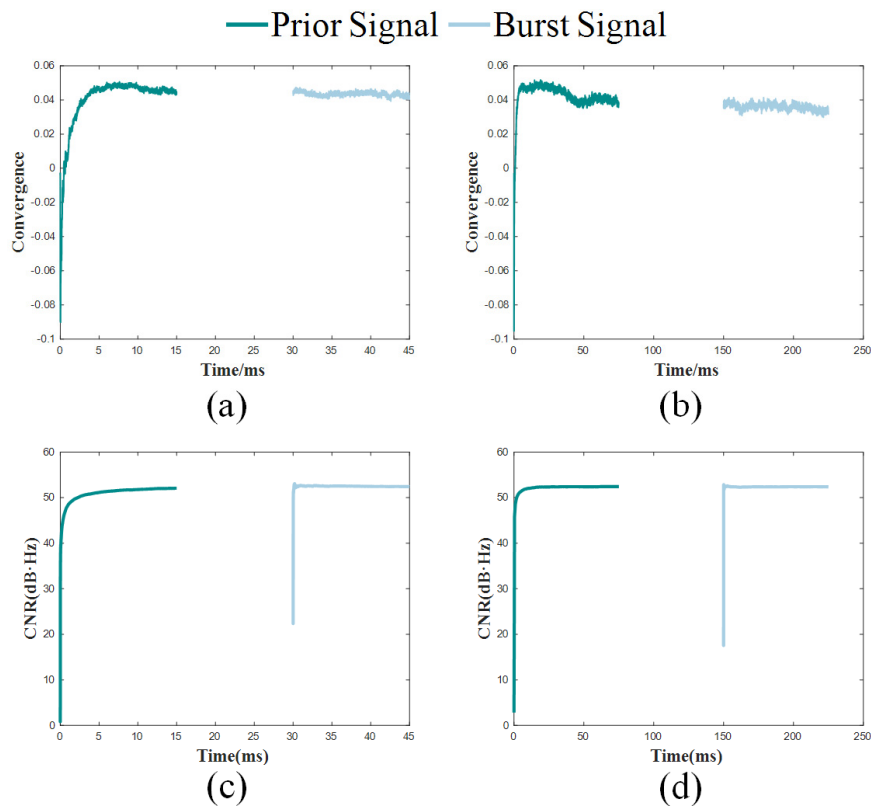
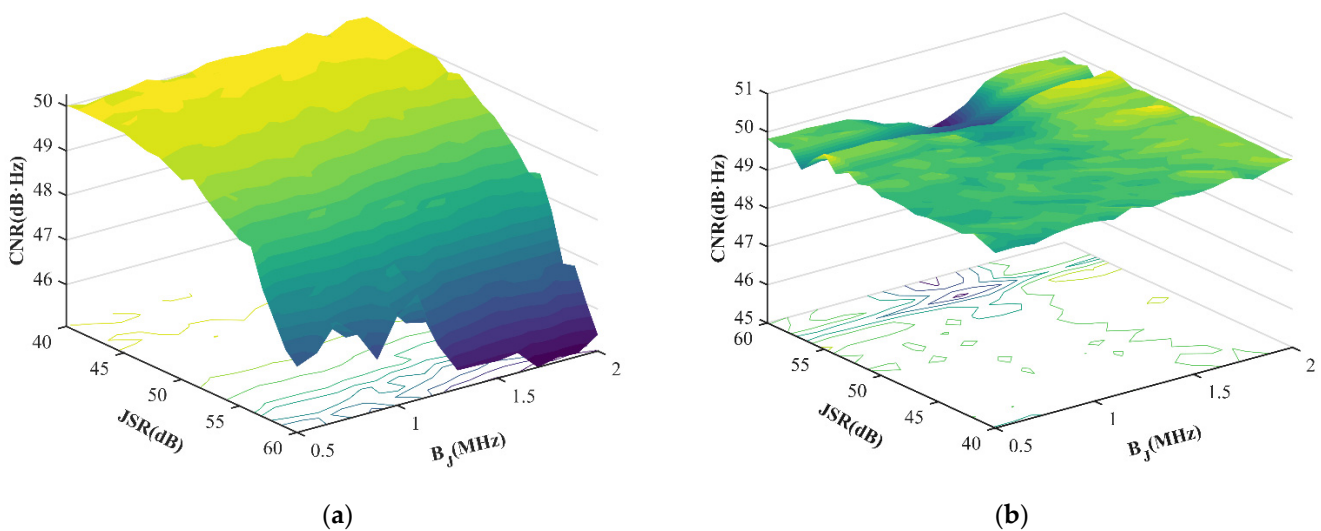


Figure 14. Performance comparison under scenarios with different signal reception intervals. (a) The convergence performance, the reception interval is 15 ms. (b) The convergence performance, the reception interval is 75 ms. (c) The interference suppression performance, the reception interval is 15 ms. (d) The interference suppression performance, the reception interval is 75 ms.

## 5. Simulation Experimental Verification

In order to verify the universal adaptability of the robust anti-jamming algorithm in navigation receivers, simulation experimental verification was performed to evaluate the performance of the navigation receiver under extensive conditions.

The robust anti-jamming algorithm is generally applicable to typical narrowband interference scenarios. Figure 15 shows that under different interference characteristics, such as intensity and bandwidth, the robust anti-interference algorithm has a noticeable improvement effect on CNR loss compared with the traditional algorithm. It is assumed that the CNR of the signal is 50 dB·Hz, the interference bandwidth is from 0.5 MHz to 2 MHz, the step is 0.1 MHz, the interference-to-signal ratio is from 40 dB to 60 dB, and the step is 1 dB. Figure 15a shows the performance of the traditional anti-jamming algorithm. As the interference-to-signal ratio increases, the CNR loss increases to 4 dB·Hz. Figure 15b shows the performance of the robust anti-jamming algorithm. The CNR loss remains stable, and the maximum CNR loss is about 1 dB·Hz.



**Figure 15.** The CNR loss under different interference characteristics. (a) The performance of the traditional anti-jamming algorithm. (b) The performance of the robust anti-jamming algorithm.

The robust anti-jamming algorithm is suitable for different signal environments and improves the receiver performance in strong signal scenarios. The performance impact of the original CNR on the data loss is more evident with a shorter signal reception interval. Figure 16 shows that the robust anti-jamming algorithm significantly improves information loss compared with the traditional algorithm under different signal power and navigation receiver receiving time slots. The CNR of the signal without interference is assumed to be 45 dB·Hz to 65 dB·Hz, covering the conventional navigation receiver environment and strong signal scenarios. The signal receiving time slot was considered from 15 ms to 1.5 s, and the data proportion of the loss information in the receiving time slot was evaluated. Figure 16a shows the performance of traditional anti-jamming algorithms. As the signal strength increases, the proportion of information loss increases, and the data loss is more pronounced in a short time slot. The proportion of information loss can be increased to 8%. Figure 16b shows the performance of the robust anti-jamming algorithm. The proportion of information loss is always below 0.1%, showing a minimal increase only in short time slots.

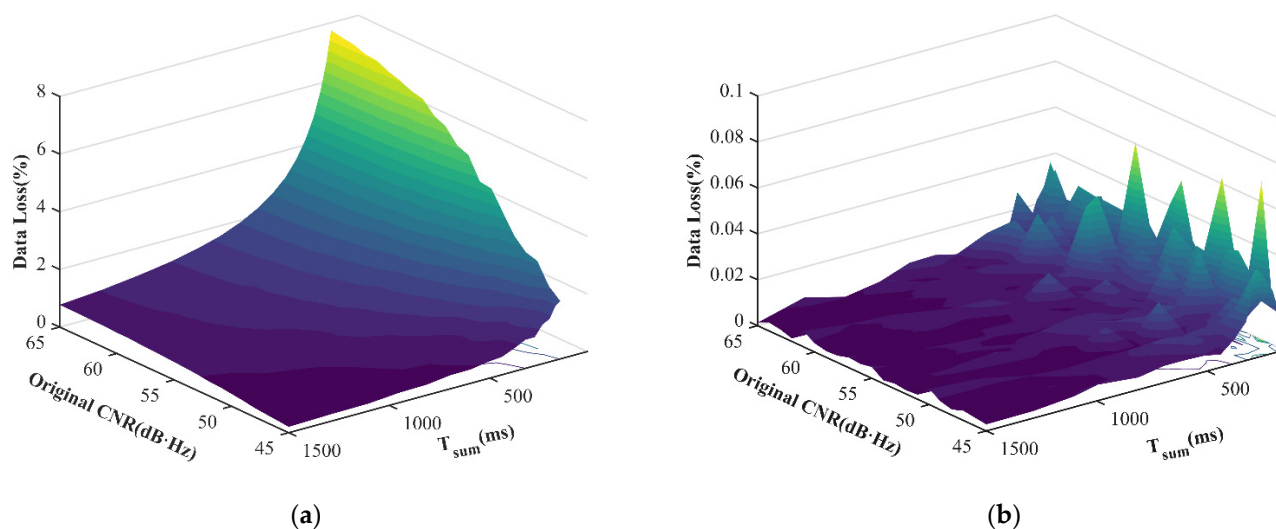


**Figure 16.** The data loss under different signal characteristics. (a) The performance of the traditional anti-jamming algorithm. (b) The performance of the robust anti-jamming algorithm.

## 6. Conclusions

Time-domain anti-jamming technology is one of the most effective ways to suppress narrowband interference. Traditional time-domain anti-jamming methods are usually used in continuous signal processing, but for T/R time-sharing reception technology the information loss caused by these methods cannot be ignored, because their long convergence time will have a great impact on the performance of the navigation receiver. This paper presents a robust anti-jamming algorithm based on T/R time-sharing technology, which can solve the information loss caused by repeated convergence of the time-domain anti-jamming filter. Based on the stability characteristics of interference, the prior weight vector is stored in memory to provide the initial value of the anti-jamming filter for the next transceiver period. The experimental results show that the CNR loss of the robust anti-jamming algorithm has been greatly improved compared with the traditional anti-jamming algorithm, and the information loss is generally 20 dB less than the traditional one. Regardless of the characteristic changes of interference and signal, the robust anti-jamming algorithm can achieve good performance improvement. In addition, the performance advantages of the robust anti-jamming algorithm may be more evident for other BeiDou link communications which are still under construction.

**Author Contributions:** B.L. (Baiyu Li) performed the theoretical study, conducted the experiments, processed the data and wrote the manuscript. Z.L. and J.S. designed the system, provided research suggestions and revised the manuscript together. W.X., J.Q. and L.H. helped in performing the experiments. Z.X. and B.L. (Baojun Lin) provided the experiment equipment and suggestions for the manuscript. All authors have read and agreed to the published version of the manuscript.

**Funding:** This research was funded by the National Natural Science Foundation of China (No.62003354).

**Institutional Review Board Statement:** Not applicable.

**Informed Consent Statement:** Not applicable.

**Acknowledgments:** The authors would like to thank the editors and reviewers for their efforts in the publication of this paper.

**Conflicts of Interest:** The authors declare no conflict of interest.

## References

1. Azmi, P.; Tavakkoli, N. Narrow-Band Interference Suppression in CDMA Spread-Spectrum Communication Systems Using Pre-Processing Based Techniques in Transform-Domain. *IEICE Trans. Commun.* **2008**, *85*, 239–246. [[CrossRef](#)]
2. Radanliev, P.; De Roure, D. New and emerging forms of data and technologies: Literature and bibliometric review. *Multimed. Tools Appl.* **2022**. [[CrossRef](#)] [[PubMed](#)]
3. Cao, L.; An, X.; Hong, G.; Guo, B. Analysis of measurement biases induced by adaptive antenna arrays for GNSS receivers. In Proceedings of the 2016 12th International Conference on Natural Computation, Fuzzy Systems and Knowledge Discovery (ICNC-FSKD), Changsha, China, 13–15 August 2016; pp. 1863–1867.
4. Lu, Z.; Nie, J.; Chen, F.; Ou, G. Impact on Antijamming Performance of Channel Mismatch in GNSS Antenna Arrays Receivers. *Int. J. Antennas Propag.* **2016**, *2016*, 1909708. [[CrossRef](#)]
5. Chien, Y.-R.; Huang, Y.-C.; Yang, D.-N.; Tsao, H.-W. A Novel Continuous Wave Interference Detectable Adaptive Notch Filter for GPS Receivers. In Proceedings of the 2010 IEEE Global Telecommunications Conference GLOBECOM 2010, Miami, FL, USA, 6–10 December 2010; pp. 1–6.
6. Du, Y.; Gao, Y.; Liu, J.; Xi, X. Frequency-Space Domain Anti-Jamming Algorithm Assisted with Probability Statistics. In Proceedings of the 2013 International Conference on Information Technology and Applications, Chengdu, China, 16–17 November 2013; pp. 5–8.
7. Fan, G.; Tang, X.; Nie, J.; Huang, Y.; Sun, G. A Zero Bias Frequency-Domain Interference Suppressor for GNSS Receivers. *IEICE Trans. Commun.* **2016**, *E99.B*, 2081–2086. [[CrossRef](#)]
8. Fan, G.T.; Zhang, F.; Ran, D.C. An unbiased carrier-phase anti-interference filter based on mirror frequency amplitude compensation. *Adv. Space Res.* **2021**, *67*, 806–811. [[CrossRef](#)]
9. Issam, S.M.; Adnane, A.; Madiabdessalam, A. Anti-Jamming techniques for aviation GNSS-based navigation systems: Survey. In Proceedings of the 2020 IEEE 2nd International Conference on Electronics, Control, Optimization and Computer Science (ICECOCS), Kenitra, Morocco, 2–3 December 2020; pp. 1–4.
10. Abdulkarim, Y.I.; Xiao, M.; Awl, H.N.; Muhammadsharif, F.F.; Lang, T.; Saeed, S.R.; Alkurt, F.O.; Bakire, M.; Karaaslan, M.; Dong, J. Simulation and Lithographic Fabrication of a Triple Band Terahertz Metamaterial Absorber Coated on Flexible Polyethylene Terephthalate Substrate. *Opt. Mater. Express* **2021**, *12*, 338–359. [[CrossRef](#)]
11. Gu, Y.; Tang, K.; Cui, H. LMS algorithm with gradient descent filter length. *IEEE Signal Process. Lett.* **2004**, *11*, 305–307. [[CrossRef](#)]
12. Hwang, S.-S. *Adaptive Algorithms for a GPS Interference Suppression Receiver and a Sparse Reconfigurable Adaptive Filter*; University of California: Santa Barbara, CA, USA, 2006.
13. Yu, X.; Yang, Q.; Xiao, Z.; Chen, H.; Havyarimana, V.; Han, Z. A Precoding Approach for Dual-Functional Radar-Communication System With One-Bit DACs. *IEEE J. Sel. Areas Commun.* **2022**, *40*, 1965–1977. [[CrossRef](#)]
14. Hao, Z.; Zhao, H.; Shao, S.; Tang, Y. Suppression of Time-varying Multi-tone Interference Based on Frequency Domain Interference Detection. *Wirel. Pers. Commun.* **2014**, *75*, 1051–1060. [[CrossRef](#)]
15. Huang, L.; Lu, Z.; Xiao, Z.; Ren, C.; Song, J.; Li, B. Suppression of Jammer Multipath in GNSS Antenna Array Receiver. *Remote Sens.* **2022**, *14*, 350. [[CrossRef](#)]
16. Dong, H.; Chi, X.F.; Liang-Dong, Q.U.; Shi, Y.W.; Zhao, X.H.; Dong, C. Anti-interference performance of TDCS based on Levinson algorithm of cross spectrum AR model parameter estimation. *J. Jilin Univ.* **2014**, *3*, 812–817.
17. Gong, Y.; Cowan, C.F.N. An LMS style variable tap-length algorithm for structure adaptation. *IEEE Trans. Signal Process.* **2005**, *53*, 2400–2407. [[CrossRef](#)]
18. Bai, Y.; Guo, Y.M.; Wang, X.; Lu, X.C. Satellite-Ground Two-Way Measuring Method and Performance Evaluation of BDS-3 Inter-Satellite Link System. *IEEE Access* **2020**, *8*, 157530–157540. [[CrossRef](#)]
19. Han, Z.Z.; Wu, Y.Z.; Liang, M.T.; Ma, Y.H.; Li, X.M. Summary of transceiver isolation technology for cw radar microstrip antenna. In Proceedings of the 2020 5th International Conference on Electromechanical Control Technology and Transportation (ICECTT 2020), Nanchang, China, 15–17 May 2020; pp. 167–171.
20. Cai, Z.W.; Han, C.H.; Du, Y.; Yang, L.; SciRes. Orbit Determination Method and Accuracy Analysis Utilizing Satellite-Ground and Satellite-Satellite Links. In Proceedings of the CSNC 2011: 2nd China Satellite Navigation Conference, Shanghai, China, 18–20 May 2011; Volume 1–3, pp. 472–476.
21. Li, X.; Chen, F.; Lu, Z.; Liu, Z.; Ou, G. Overview of Anti-Jamming Technology Based on GNSS Single-Antenna Receiver. In Proceedings of the 2020 3rd International Conference on Geoinformatics and Data Analysis, Marseille, France, 15–17 April 2020; pp. 96–104.
22. McGraw, G.A.; McDowell, C.; Young, R.S.Y.; Glessner, D.W. Assessment of GPS anti-jam system pseudorange and carrier phase measurement error effects. In Proceedings of the 18th International Technical Meeting of the Satellite Division of The Institute of Navigation, ION GNSS 2005, Long Beach, CA, USA, 13–16 September 2005; pp. 603–607.
23. Lu, Z.; Nie, J.; Chen, F.; Chen, H.; Ou, G. Adaptive Time Taps of STAP Under Channel Mismatch for GNSS Antenna Arrays. *IEEE Trans. Instrum. Meas.* **2017**, *66*, 2813–2824. [[CrossRef](#)]
24. Widrow, B.; McCool, J.M.; Larimore, M.G.; Johnson, C.R. Stationary and nonstationary learning characteristics of the LMS adaptive filter. *Proc. IEEE* **1976**, *64*, 1151–1162. [[CrossRef](#)]

25. Luo, Z.J.; Zhao, L.; Chen, D.B.; Xue, C.J.; Wu, S.Y. Optimizing Effect of the High-Impedance Surface on Radiation Performances of the Vlasov Launcher. In Proceedings of the 2017 IEEE Asia Pacific Microwave Conference (APMC), Kuala Lumpur, Malaysia, 13–16 November 2017; pp. 349–352.
26. Zhao, L.Q.; Hu, X.G.; Tang, C.P.; Zhou, S.S.; Cao, Y.L.; Wang, Q.X.; Su, R.R. Inter-satellite link augmented BeiDou-3 orbit determination for precise point positioning. *Chin. J. Aeronaut.* **2022**, *35*, 332–343. [[CrossRef](#)]
27. Yang, W.K.; Gong, H.; Liu, Z.J.; Li, Y.L.; Sun, G.F. Improved two-way satellite time and frequency transfer with Multi-GEO in BeiDou navigation system. *Sci. China-Inf. Sci.* **2014**, *57*, 1–15. [[CrossRef](#)]
28. Lu, Z.; Nie, J.; Wan, Y.; Gang, O. Optimal reference element for interference suppression in GNSS antenna arrays under channel mismatch. *IET Radar Sonar Navig.* **2017**, *11*, 1161–1169. [[CrossRef](#)]
29. Ketchum, J.; Proakis, J. Adaptive Algorithms for Estimating and Suppressing Narrow-Band Interference in PN Spread-Spectrum Systems. *IEEE Trans. Commun.* **1982**, *30*, 913–924. [[CrossRef](#)]
30. Song, J.; Lu, Z.; Xiao, Z.; Li, B.; Sun, G. Optimal Order of Time-Domain Adaptive Filter for Anti-Jamming Navigation Receiver. *Remote Sens.* **2022**, *14*, 48. [[CrossRef](#)]
31. Mammela, A. The performance of adaptive interference suppression filters used in PN spread-spectrum systems. In Proceedings of the 8th European Conference on Electrotechnics, Conference Proceedings on Area Communication, Stockholm, Sweden, 13–17 June 1988; pp. 126–129.
32. Wang, J.; Peng, J.; Xu, X.; You, X.; Liu, S. A single-input Narrow-band Interference Suppression and Smoothing Algorithm Based on LMS Filter. In Proceedings of the 2019 IEEE 2nd International Conference on Electronic Information and Communication Technology (ICEICT), Harbin, China, 20–22 January 2019; pp. 192–198.
33. Lu, Z.; Song, J.; Huang, L.; Ren, C.; Xiao, Z.; Li, B. Distortionless 1/2 Overlap Windowing in Frequency Domain Anti-Jamming of Satellite Navigation Receivers. *Remote Sens.* **2022**, *14*, 1801. [[CrossRef](#)]
34. Wei, Y.; Yan, Z. Variable Tap-Length LMS Algorithm with Adaptive Step Size. *Circuits Syst. Signal Process.* **2017**, *36*, 2815–2827. [[CrossRef](#)]
35. Zhong, W. Linear Phase FIR Digital Filter Design Using Differential Evolution Algorithms. Master's Thesis, University of Windsor, Windsor, ON, Canada, 2017.
36. Kwong, R.H.; Johnston, E.W. A variable step size LMS algorithm. *IEEE Trans. Signal Process.* **1992**, *40*, 1633–1642. [[CrossRef](#)]
37. Shin, H.-C.; Sayed, A.H.; Song, W.-J. Variable step-size NLMS and affine projection algorithms. *IEEE Signal Process. Lett.* **2004**, *11*, 132–135. [[CrossRef](#)]
38. Wang, B.; Sun, Y.J.; Liu, Y.; Zhang, Y.Z.; Li, S. Experimental Research on Narrowband Interference Suppression of GNSS Signals. *Wirel. Commun. Mob. Comput.* **2021**, *2021*, 3410741. [[CrossRef](#)]
39. Yasyukevich, Y.V.; Yasyukevich, A.S.; Astafyeva, E.I. How modernized and strengthened GPS signals enhance the system performance during solar radio bursts. *GPS Solut.* **2021**, *25*, 46. [[CrossRef](#)]
40. Shu, Y.M.; Fang, R.X.; Liu, J.N. Stochastic Models of Very High-Rate (50 Hz) GPS/BeiDou Code and Phase Observations. *Remote Sens.* **2017**, *9*, 1188. [[CrossRef](#)]
41. Li, H.; Huo, Q.; Zheng, X.; Yan, S.; He, Y. High Dynamic GNSS Anti-jamming Algorithms Based on Nulling Widening and Deepening. In Proceedings of the 2020 IEEE 4th Information Technology, Networking, Electronic and Automation Control Conference (ITNEC), Chongqing, China, 12–14 June 2020; pp. 1562–1568.